

Tighter Control of Quantum Cascade Laser Frequency Combs with
an Optical Phase-Locked Loop

Audrey Zeng

April 29, 2025

Advisor: Gerard Wysocki

Submitted in partial fulfillment

of the requirements for the degree of

Bachelor of Science in Engineering

Department of Electrical and Computer Engineering

Princeton University

I hereby declare that this Independent Work report represents my own work in accordance
with University regulations.

I hereby declare that this Independent Work report does not include regulated human
subjects research.

I hereby declare that this Independent Work report does not include regulated animal
subjects research.

A handwritten signature in black ink, appearing to read "Audrey Zeng", is written over a small rectangular box.

Audrey Zeng

Tighter Control of Quantum Cascade Laser Frequency Combs with an Optical Phase-Locked Loop

Audrey Zeng

Quantum Cascade Lasers (QCLs) are promising broadband spectroscopy tools for their ability to generate optical frequency combs (FCs) in the mid-infrared range. However, their usability is hindered by unstable performance and susceptibility to optical feedback. Previously, I demonstrated stabilization of a comb's two degrees of freedom – repetition rate frequency (f_{rep}) and carrier envelope offset frequency (f_{ceo}) – through injection of an external amplitude modulated radio frequency (AM-RF) signal at frequency of f_{rep} of the free-running QCL-FC. However, the comb's f_{ceo} fluctuated much more at smaller integration times less than 1 second, indicating the need for a more efficient control loop able to stabilize comb performance on smaller time scales. An optical phase-locked loop (OPLL) was proposed for its efficiency; additionally, commercially available OPLL systems such as Toptica's mFALC 110 allow OPLL integration to be a seamless process with relatively few optical components needed. This project determined the workings of the mFALC 110's OPLL and high-speed linear control amplifier circuit and characterized its frequency response. Because the mFALC 110 has a high bandwidth but small holding range, it was determined that a double locking loop – with the existing frequency discriminator circuit providing "slow" locking of f_{ceo} and the OPLL providing "fast" locking – would be most effective. Thus, the resulting design combined the existing control loop with the frequency discriminator circuit controlling amplitude modulation of the external RF injection, and added in the OPLL to modulate the QCL-FC driver current based on fluctuations in f_{ceo} .

ACKNOWLEDGMENTS

Much of this semester was dedicated to learning how to learn theory (about control loops, PID controllers, PLLs and OPLLs), and how to design productive experiments (learning how to characterize control loops). I've grown both as a theorist and experimentalist, lessons which would not have been possible without the dedicated mentorship of those around me. Thank you to Professor Gerard Wysocki for all his patience, guidance, and teaching. Thank you to Baichuan Huang for his extremely generous mentorship over the past year; without him, I would not be the scientist, student, or electrical engineer whom I am today. Also, thank you to the rest of the members of the PULSe lab: Nick, Nishant, and Brady, for their kindness and support and for making the lab a fun environment to be in.

Contents

1	Introduction	6
2	Background	7
2.1	Previous QCL-FC Stabilization Work	7
3	Phase-Locked Loops	11
3.1	Optical Phase-Locked Loops	12
4	OPLL Investigation	13
4.1	mFALC 110 Operation	13
4.2	OPLL Characterization	14
5	Proposed Implementation	17
6	Conclusions	20

1 Introduction

Optical frequency combs (OFCs) refer to broadband radiation sources consisting of equally-spaced, phase-locked modes [1, 2]. Because OFCs emit signals at a range of known frequencies, they are promising tools for broadband spectroscopy. There has been much interest in OFC sources with emissions in the mid-infrared range, which contains the rotational-vibrational modes of many gas molecules of interest. OFCs generated by Quantum Cascade Lasers, or Quantum Cascade Laser-Frequency Combs (QCL-FCs), are one such example of mid-infrared OFCs. QCL-FCs are additionally attractive for their capability for self-starting comb generation, where comb generators are chip scale and require only electrical pumping as opposed to larger, more complex optical systems [3, 4].

However, despite their advantages, free-running QCL-FCs remain extremely sensitive to optical feedback, and reproducing comb performance remains a challenge. Comb performance can be characterized by looking at the comb's two degrees of freedom: the repetition rate frequency and carrier envelope offset frequency. A comb's repetition rate frequency (f_{rep}) is the difference in frequency between adjacent lines, which manifests the comb's relative phase stability. The carrier envelope offset frequency (f_{ceo}) refers to the frequency of the first comb line, which indicates the comb's absolute phase stability. Knowing only these two degrees of freedom, each comb mode f_n can be calculated with the formula:

$$f_n = f_{ceo} + n f_{rep}$$

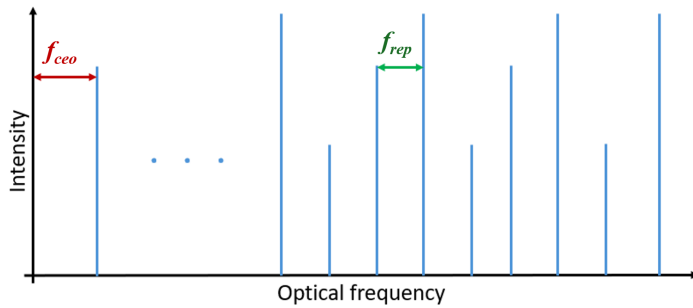


Figure 1: A simplified representation of a QCL spectrum in the frequency domain. The carrier envelope offset frequency, or f_{ceo} (the frequency of the first comb mode) and the repetition rate frequency, or f_{rep} (the frequency difference between adjacent comb lines) are shown.

Stable comb states for QCL-FCs are difficult to reproduce because maintaining specific f_{ceo} and f_{rep} values is difficult. Thus, external stabilization methods have been of great interest. The locking mechanism of interest to this project was first demonstrated by Hillbrand et al., who showed successful control of f_{rep} with only an external radio frequency (RF) injection at frequency f_{rep} [5]. As opposed to other control methods, which commonly involve locking the frequency comb to an external optical comb, control with only an external RF injection is simple and is a promising method for deployable applications [6, 7, 8]. Control of f_{rep} with an RF injection was already established, and last semester, our lab was able to successfully demonstrate control of the QCL-FC's f_{ceo} value with the same external RF injection at f_{rep} by modulating the amplitude of the injected signal. However, f_{ceo} was significantly more stable over long time periods, while stability over short time periods (<1 second) was much higher, indicating that our existing control loop was unable to successfully prevent fast, short-term fluctuations to the same degree as long-term ones. To increase f_{ceo} stability on shorter time scales, a fast locking loop was needed. Thus, this project investigated the use of an optical phase-locked loop (OPLL) to provide this efficient locking loop.

2 Background

2.1 Previous QCL-FC Stabilization Work

f_{ceo} was previously stabilized by adding amplitude modulation to the external RF injection signal. The desired amplitude modulation would have a depth proportional to the fluctuations in frequency of f_{ceo} , necessitating the design of a control loop to detect the frequency fluctuations of f_{ceo} and adjust the amplitude modulation accordingly. The control loop design (Fig. 2) was partially inspired by the “daisy-chain” frequency stabilization setup by Liu et al. for a deployable dual-comb spectroscopy system [9].

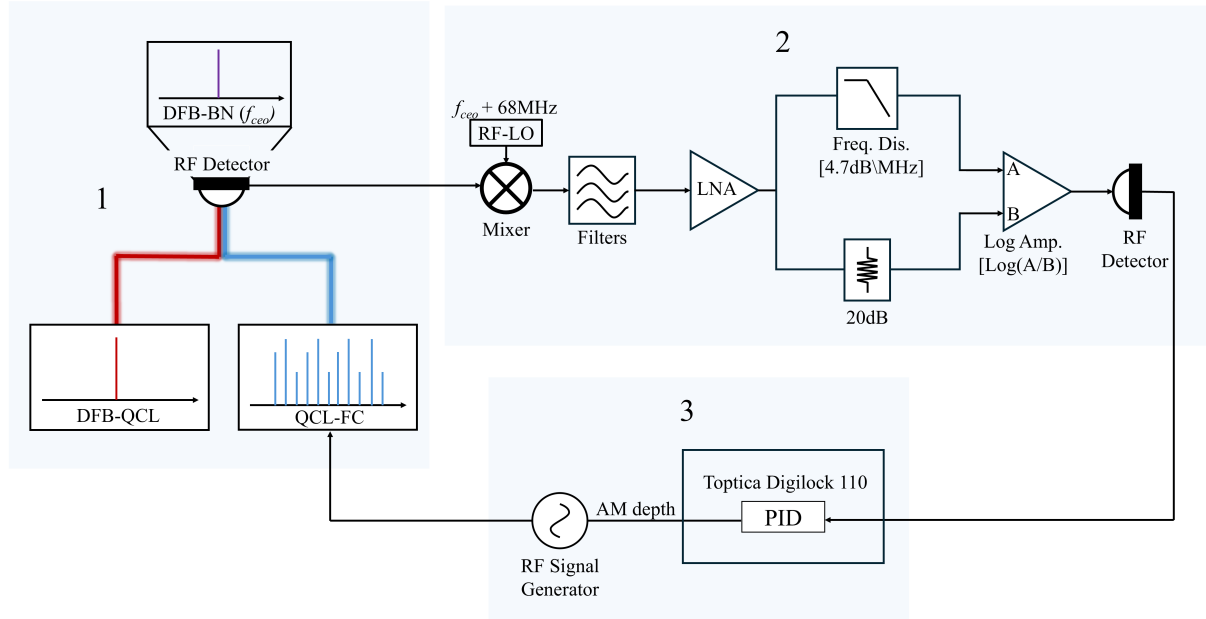


Figure 2: The control loop previously used to stabilize f_{ceo} . First, a proxy signal for f_{ceo} , called the DFB-BN, is generated by sending the outputs of a DFB-QCL and QCL-FC into the same RF detector. The DFB-BN signal is mixed down and sent to a frequency discriminator to convert frequency fluctuations to intensity fluctuations, outputting a frequency-dependent error signal. This error signal is sent to a PID controller, which controls the amplitude modulation depth of the external RF injection signal to decrease f_{ceo} fluctuations.

The stabilization control loop is divided into three main parts, indicated by the blue boxes in Fig. 2.

Part 1 demonstrates how f_{ceo} is measured. Signals from the QCL-FC and a single-mode distributed-feedback QCL (DFB-QCL) are sent to the same RF detector. The DFB-QCL mode beats with the comb lines of the QCL-FC, producing a signal at the difference frequency between the DFB-QCL and the nearest modes of the QCL-FC (Fig. 3). This signal is notated as the DFB beat note (DFB-BN). The DFB-BN acts as a proxy signal for the frequency of f_{ceo} : as f_{ceo} fluctuates, the difference frequency between the DFB-QCL and QCL-FC mode changes, thus shifting the DFB-BN signal proportionally.

Part 2 is the frequency discriminator circuit which converts frequency fluctuations of the DFB-BN to intensity fluctuations. The DFB-BN signal is first mixed with a local oscillator (RF-LO) signal that has frequency 68 MHz higher than the DFB-BN signal frequency, producing a mixer output signal with frequency

68 MHz (a frequency on the slope of the frequency discriminator). The mixed down signal is sent through filters and a low noise amplifier (LNA) to increase the signal-to-noise ratio before being fed to the frequency discriminator. This output is sent to a log amplifier alongside a 20 dB offset intensity to prevent intensity fluctuations of f_{ceo} from being interpreted as fluctuations in the DFB-BN frequency. The resulting output signal of the log amp is used as an error signal.

In part 3, the aforementioned error signal is sent to a PID controller (integrated into a Toptica Digilock 110 module). The PID controller outputs a voltage dependent on the error signal from part 2, controlling the amplitude modulation depth of the injected RF signal correspondingly, closing the control loop.

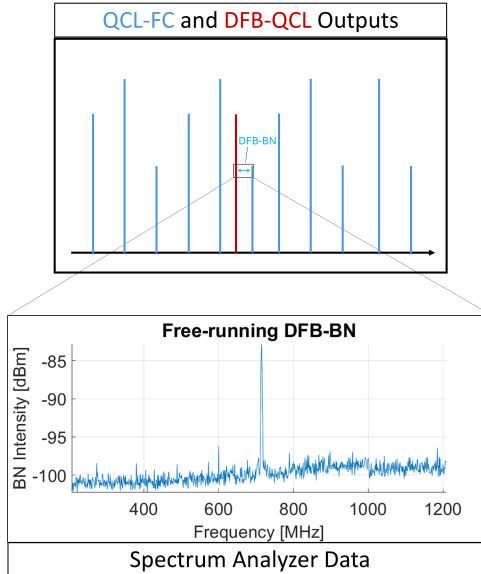


Figure 3: Generation of the DFB-BN, a proxy signal for f_{ceo} . The top box is a simplified representation of the spectra of the QCL-FC and DFB-QCL. The single comb mode of a DFB-QCL (the red spectrum) beats with the closest comb mode of the QCL-FC (the blue spectrum), to produce a DFB-BN signal at the frequency of their difference, as shown in the spectrum analyzer data in the bottom box.

Fluctuations of f_{ceo} over time were quantified by calculating the Allan deviation [10]. Allan deviation is the square root of Allan variance, or two-sample variance. Allan variance is dependent on the time period between the two samples, hence its representation as a graph rather than one value. For a given integration time, the Allan variance can be understood as the relative root mean square value between two samples separated by the specified integration time.

When the QCL-FC was operated with an amplitude-modulated RF injection controlled by this loop, f_{ceo} frequency fluctuations decreased significantly. While the Allan deviation of f_{ceo} was roughly the same when the comb was free-running and injected with an unmodulated RF signal at frequency f_{rep} , the Allan deviation of f_{ceo} when the laser was injected with the amplitude-modulated RF signal decreased by an order of magnitude (Fig. 3).

Though Allan deviation values decreased overall with the amplitude-modulated injection signal, there is still room for greater stabilization for lower integration times, highlighted in green in Fig. 4. The Allan deviation values for these lower integration times remained significantly higher than the deviation values for higher integration times, indicating that short-term stability of f_{ceo} could still be improved. This necessitates a more efficient control loop to react faster to fluctuations in f_{ceo} . Ideally, the new control loop to be implemented would be efficient enough to achieve Allan deviation values as low as 10^{-1} for integration times on the order of magnitude of hundreds of μs . One such possibility for a more efficient control loop is the use of a optical phase-locked loop (OPLL).

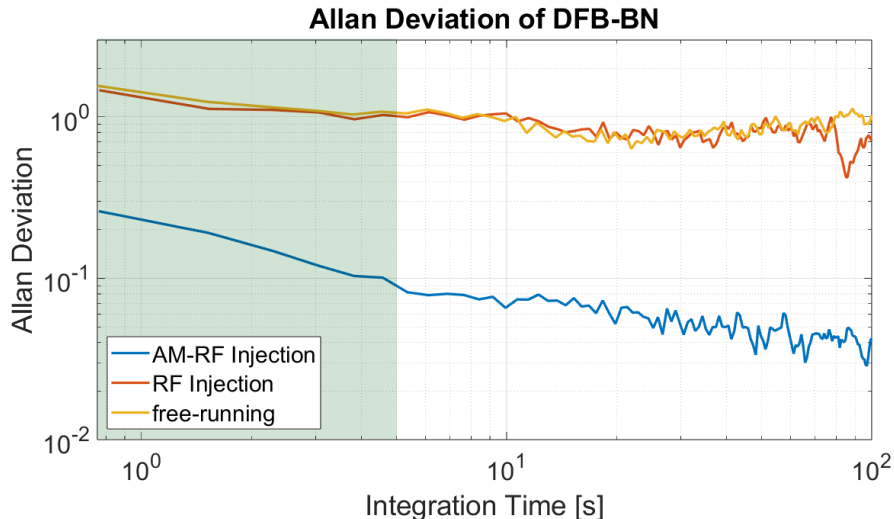


Figure 4: Allan deviation of f_{ceo} frequency when the QCL-FC is free-running, is injected with an unmodulated RF signal at frequency f_{rep} , and when it is injected with an amplitude-modulated RF signal at frequency f_{rep} . The Allan deviation for lower integration times, highlighted in green, could be improved

3 Phase-Locked Loops

A phase-locked loop (PLL) is an efficient control loop which outputs a signal whose phase (and therefore, also frequency) matches that of a provided reference input signal. A basic PLL circuit consists of 3 components: a phase detector, a low-pass filter, and a voltage-controlled oscillator (VCO) (Fig. 5).

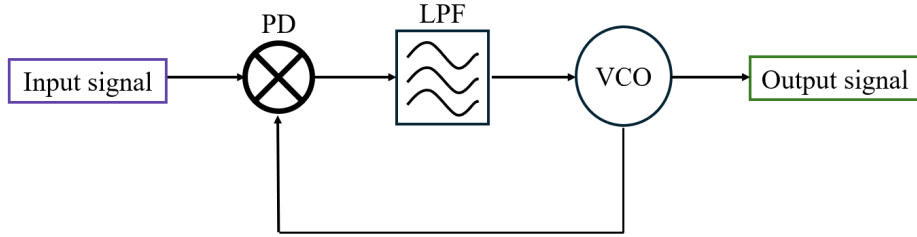


Figure 5: A basic PLL circuit. The input signal is fed to a phase detector (PD). The phase detector output is then filtered by a low pass loop filter (LPF), before being fed to the voltage controlled oscillator (VCO), which generates an output signal also fed into the PD.

The phase detector detects the difference in phase between the input signal and the output signal generated by the VCO. Phase detectors commonly use a multiplier circuit to output signals representing the phase difference: given two signals with phases ϕ_1 and ϕ_2 and assuming the phase difference is small, the phase detector will produce the following output:

$$\sin \phi_1 \cos \phi_2 = \frac{\sin(\phi_1 - \phi_2)}{2} + \frac{\sin(\phi_1 + \phi_2)}{2} \approx \frac{\phi_1 - \phi_2}{2} + \frac{\sin(\phi_1 + \phi_2)}{2}$$

The second sinusoidal term is filtered out, leaving only the desired phase difference as the output voltage. This output is then passed to the loop filter (LPF), which helps determine loop dynamics and limits unwanted outputs from the phase detector. The filter output is passed to the VCO, which generates a signal whose frequency depends on the input voltage [11]. The VCO output is fed back into the PD for further phase comparison with the reference signal until the phase difference is 0. When the difference becomes negligible, the PLL is "locked," and the frequency and phase of the output signal match that of the input signal.

3.1 Optical Phase-Locked Loops

Optical phase-locked loops (OPLLs) are PLLs where the input and output signals are optical, such as in Fig. 6. Since the goal of this project is to control the frequency of a laser, an OPLL was used.

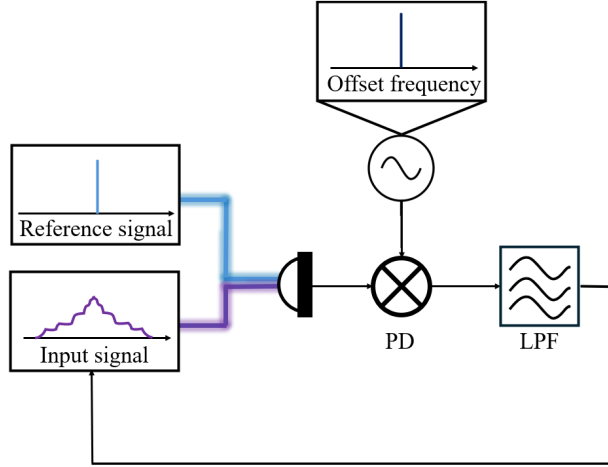


Figure 6: A basic heterodyne OPLL circuit. An input signal is sent to a detector, then fed to a phase detector (PD) along with a reference signal at the desired frequency of the input signal. The PD output it sent through a loop filter (LPF) before being fed back into the driver of the input signal.

A heterodyne OPLL uses two lasers to lock one: the laser of interest. The laser of interest (commonly referred to as the “slave laser”, but in our case, the DFB-BN) provides the input signal, and the other (the “master laser,” for this project: a generated LO signal) provides a reference signal at the desired locking frequency. The two laser outputs are sent to an optical detector, whose output is fed to a phase detector, similar to a PLL. The phase detector can also incorporate an additional input signal at the desired frequency difference between the reference and input signal (the offset frequency). The PD output is sent to the loop filter. The filter output is then sent back to the input signal laser driver to lock the input signal [12]. OPLLs provide efficient locking of the input signal, making them a desirable choice of control loop for the intended goal of improving locking for shorter time frames. Additionally, commercially available OPLL modules, such the Toptica mFALC 110, combine both an OPLL and controller circuit into one unit, making an OPLL a convenient and cost-efficient method to integrate into the QCL-FC control loop.

4 OPLL Investigation

4.1 mFALC 110 Operation

In order to determine how to use an OPLL to control f_{ceo} , the operation of the Toptica mFALC 110 module, the chosen OPLL component, had to be understood. The module consists of an analog RF phase detector and a high-speed, linear PID controller, with inputs, outputs, and PID controller settings accessible from the module's front panel (Fig. 7).

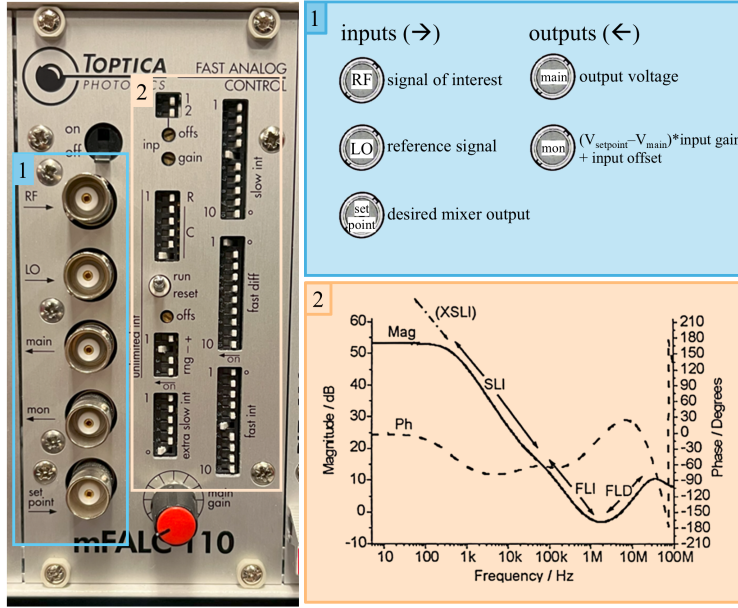


Figure 7: The front panel of the mFALC 100, split into 2 groups of components. Box 1 indicates the function of each port. Box 2 is a Bode plot explaining how each group of pins affects the response of the internal PID controller.

The module has 3 input ports. The RF input port is for the signal of interest, and the LO input port is for the reference signal which the signal of interest is to be locked. Inputs from the RF and LO ports are sent to the internal analog RF mixer for phase detection, then sent to the PID controller circuit, which outputs a frequency-dependent error signal at the main output port. The monitor output port is the difference between the setpoint and main outputs accounting for input gain and offset, and is described by the following equation:

$$(V_{setpoint} - V_{main}) * \text{input gain} + \text{input offset}$$

The monitor output port is meant primarily for viewing the phase error signal on an oscilloscope. The set

point input is used to set the desired frequency difference between the RF and LO signals.

The transfer function of the module's internal high-speed control circuit can be adjusted through pins on the front panel. Each group of pins controls the slopes of the magnitude and phase response for a given subset of frequencies, as shown in box 2 of Fig. 7. The main gain knob below the pins can tune the gain of the main output from 0 to $\pm 2V$.

4.2 OPLL Characterization

After determining the module's capabilities, its frequency response was characterized. The main goal was to determine the OPLL's holding range, or how large the frequency difference between the RF and LO signals could be in order for the OPLL to still lock the RF signal. To experimentally determine the locking range, the module was set up as shown in Fig. 8.

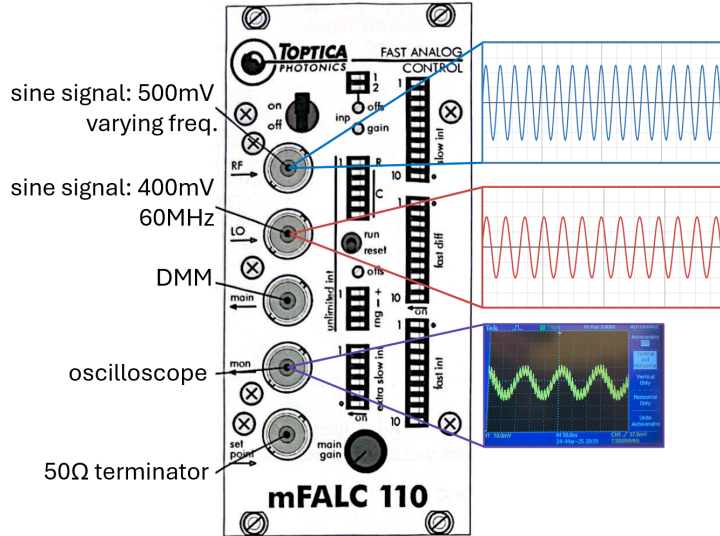


Figure 8: The module setup to determine holding range. A reference sine signal with amplitude 400 mV and frequency 60 MHz was inputted into the LO input port. The RF input port was fed a 500 mV sine signal whose frequency was tuned up and down from 60 MHz to determine when the output voltage (measured with a DMM from the main output port) stopped changing proportionally to changes in the RF input frequency. An oscilloscope was connected to the monitor port to monitor the error signal, and a 50Ω terminator connected to the set point input, as no set point frequency was desired.

Function generators (Tektronix AFG3102) were used to generate sinusoidal inputs for the RF and LO

input ports. A digital multimeter (DMM) was connected to the main output port to monitor the voltage's frequency response. An oscilloscope was connected to the monitor output port for additional confirmation of the voltage shown on the DMM. A $50\ \Omega$ terminator was connected to the set point input to prevent unwanted impedance mismatches and indicate to the OPLL to lock the RF signal to the exact frequency of the LO signal. The LO signal was set as a 400 mV sinusoidal signal at frequency 60 MHz. The RF input was a 500 mV sinusoidal signal. Its frequencies were tuned both up and down from 60 MHz at step sizes of 5 kHz and 1 kHz, and the voltage of the main output port was monitored. The results are shown in Fig. 9.

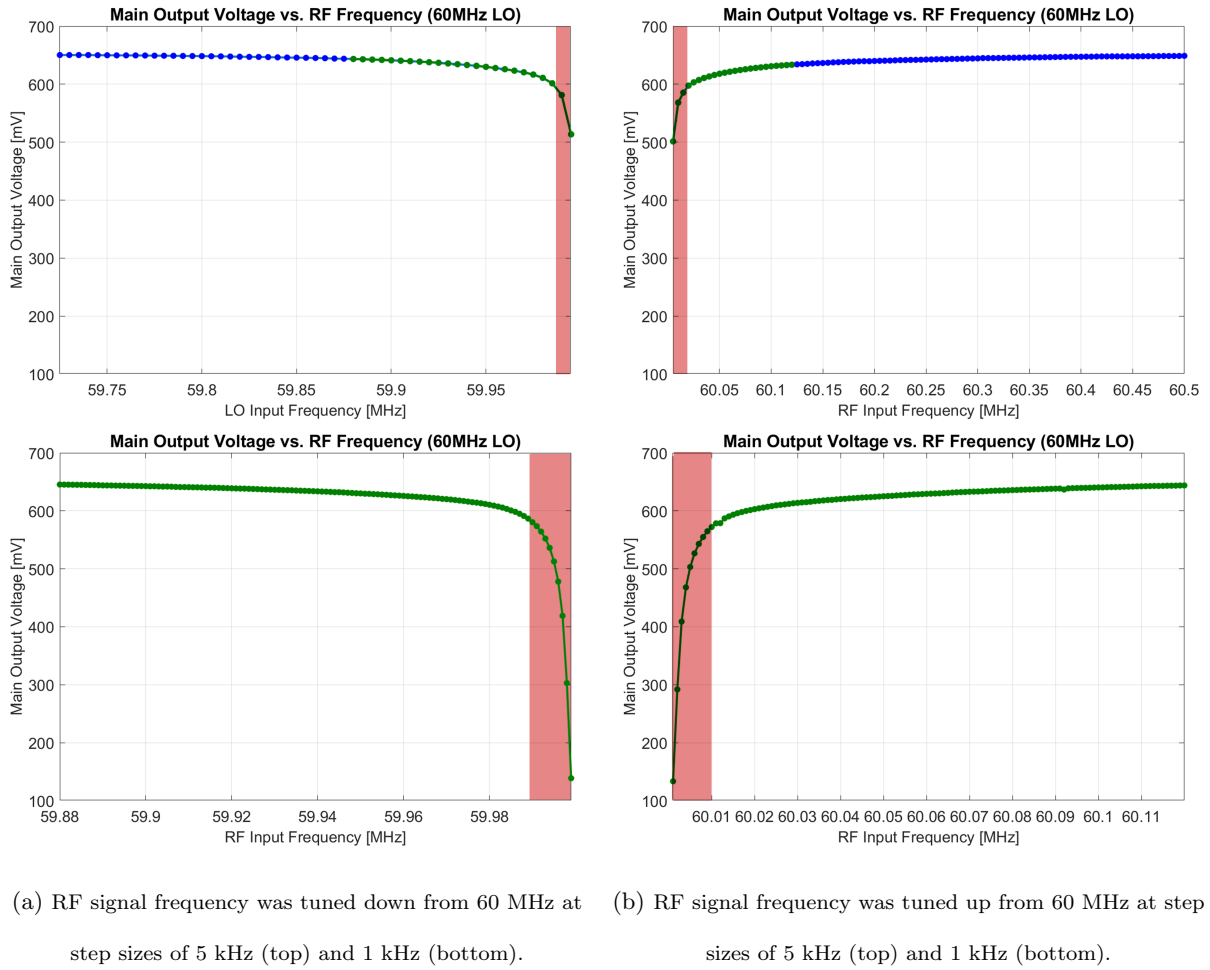


Figure 9: Frequency Response of the mFALC 110 module for a LO signal with frequency 60 MHz. The holding range (roughly 10 kHz) is highlighted in red.

The holding range of the OPLL is the range at which the main voltage output changes proportionally to

the input RF frequency. For when the RF signal had a frequency both below and above that of the LO signal, the holding range was around 10 kHz. Since f_{ceo} of our QCL-FC can drift as much as 10 kHz in less than a minute, it is insufficient to implement the OPLL on its own to lock f_{ceo} . Partially inspired by the work of Westberg et. al, it was decided to instead propose a stabilization method with two control loops: the frequency discriminator circuit discussed previously and the OPLL [13]. The frequency discriminator circuit would stabilize f_{ceo} for it to fall within the locking range of the OPLL, which would then provide the efficient high-speed locking originally desired.

5 Proposed Implementation

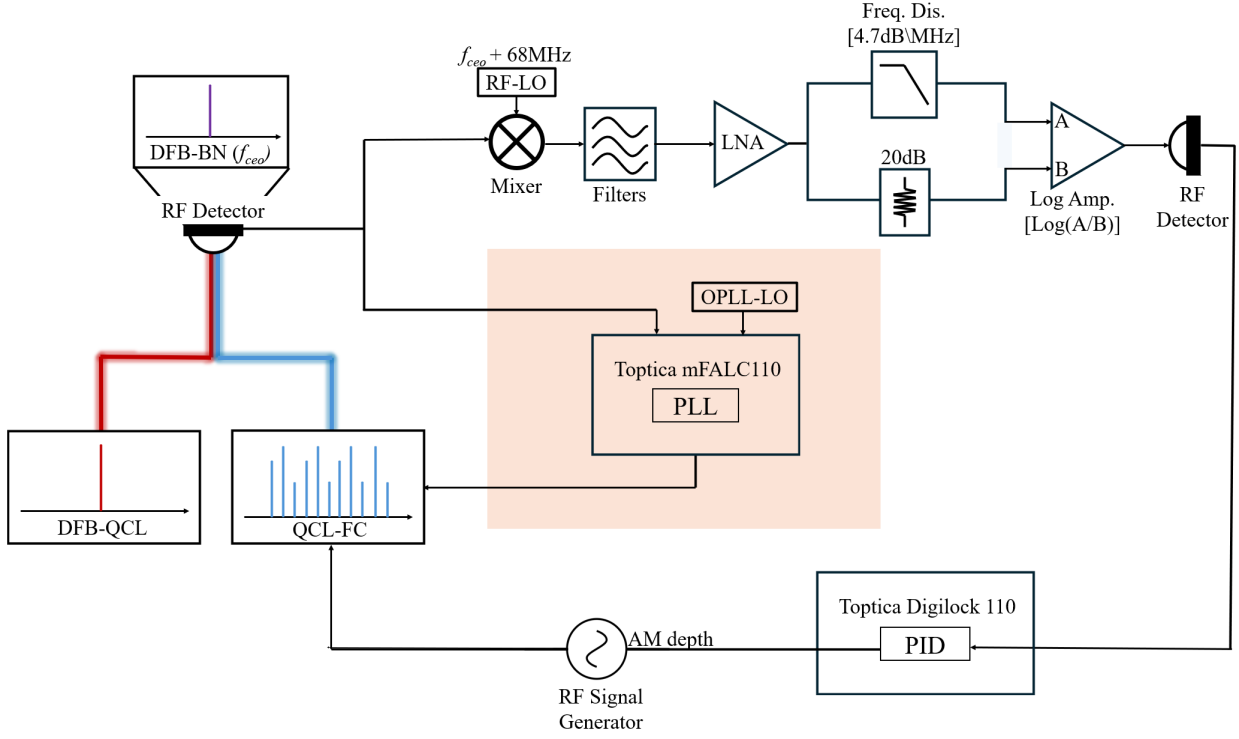


Figure 10: The double control loop to stabilize the QCL-FC. The slow frequency discriminator control loop was kept to modulate the amplitude modulation depth of the external RF injection, which has bandwidth of $<100\text{ kHz}$. The bandwidth of the QCL-FC driver is larger at $<2\text{-}3\text{ MHz}$. Thus, the output of the OPLL, which provides faster locking, is to be connected to the laser driver to modulate laser driver current. The DFB-BN signal and a local oscillator reference signal (OPLL-LO) would be fed into the OPLL for locking.

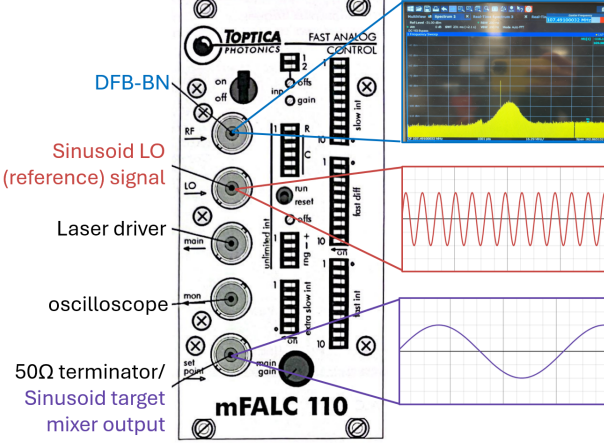


Figure 11: mFALC 110 setup for locking. The DFB-BN signal would go to the RF input port. An externally generated LO signal, whose frequency is determined by the DFB-BN frequency after it is stabilized by the slow locking loop, is fed into the LO input port. The main output port would be connected to the QCL-FC driver. Depending on the desired setpoint frequency, a terminator or sinusoidal signal would be inputted into the set point input port.

Fig. 10 shows the proposed implementation of the double control loop; the frequency discriminator loop would provide slower locking of the laser, stabilizing it enough for the OPLL to provide faster locking. Fig. 11 shows the corresponding proposed setup of the mFALC 110. The DFB-BN detected by the RF detector is sent to both the mixer in the frequency discriminator circuit (as before), and the RF port of the mFALC 110. An additional reference signal, denoted the OPLL-LO, will be generated and fed into the LO port of the mFALC 110. The frequency of the OPLL-LO would be determined by the initially stabilized frequency of the DFB-BN after applying control by the frequency discriminator circuit. The main output port of the mFALC 110 would be connected to the QCL-FC driver to modulate the laser driver current, as the laser driver has a larger bandwidth of <2-3 MHz. The injected RF signal's amplitude modulation depth, with a smaller bandwidth of <100 kHz, is still to be modulated by the previously implemented frequency discriminator circuit. The monitor output port would be connected to an oscilloscope for monitoring, and the setpoint input would be connected to a 50Ω terminator (if the DFB-BN is to be locked to the frequency of the OPLL-LO input exactly) or an additional sinusoidal input of a desired frequency difference between the DFB-BN and OPLL-LO.

By combining the frequency discriminator control loop with an OPLL, this new control loop would continue to provide the successful control demonstrated previously with just the frequency discriminator circuit, while also improving locking efficiency on shorter-time scales, thus improving the overall stability and performance of the QCL-FC.

6 Conclusions

This project has thus demonstrated the design of a double-locking scheme integrating an OPLL circuit to increase the locking efficiency of a QCL-FC. A tight lock of f_{rep} by injecting an external RF signal at the frequency of f_{rep} has already been established. We previously also successfully locked f_{ceo} by controlling the amplitude modulation depth of the external RF injection through closed-loop control with a frequency discriminator circuit. This control loop was able to decrease the Allan deviation of f_{ceo} by an order of magnitude for integration times above an order of magnitude of 10^0 .

The goal of this project was to design a control loop to increase the short-term stability of f_{ceo} , meaning a decrease in Allan deviation values for smaller integration times up to hundreds of μs . By characterizing an already available OPLL unit and investigating its capabilities and limitations through reading literature and experimentally determining its frequency response, it was determined that the OPLL could be successfully integrated with the existing frequency discriminator control loop, creating a double control loop which would provide the desired high locking efficiency.

The main limitation to this design lies in the ability of the OPLL to lock broad signals with high full width half maximum (FWHM) values. The DFB-BN of our QCL-FC can have FWHM values of up to 20 kHz, which is greater than the efficient holding range of the OPLL. The eventual implementation of the proposed control loop can provide insight into whether or not any further modification to the control loops are necessary to best handle high FWHM values.

Despite this limitation, the proposed control loop remains a promising method to further stabilize QCL-FCs to be more efficient and viable for various broadband spectroscopy applications.

References

- [1] Th Udem, R. Holzwarth, and T. W. Hänsch. “Optical frequency metrology”. en. In: *Nature* 416.6877 (Mar. 2002). Publisher: Nature Publishing Group, pp. 233–237. ISSN: 1476-4687. DOI: 10.1038/416233a. URL: <https://www.nature.com/articles/416233a> (visited on 12/06/2024).
- [2] Nathalie Picqué and Theodor W. Hänsch. “Frequency comb spectroscopy”. en. In: *Nature Photonics* 13.3 (Mar. 2019). Publisher: Nature Publishing Group, pp. 146–157. ISSN: 1749-4893. DOI: 10.1038/s41566-018-0347-5. URL: <https://www.nature.com/articles/s41566-018-0347-5> (visited on 12/06/2024).
- [3] Dmitry Kazakov et al. “Self-starting harmonic frequency comb generation in a quantum cascade laser”. en. In: *Nature Photonics* 11.12 (Dec. 2017), pp. 789–792. ISSN: 1749-4885, 1749-4893. DOI: 10.1038/s41566-017-0026-y. URL: <https://www.nature.com/articles/s41566-017-0026-y> (visited on 04/29/2025).
- [4] Andreas Hugi et al. “Mid-infrared frequency comb based on a quantum cascade laser”. en. In: *Nature* 492.7428 (Dec. 2012). Number: 7428 Publisher: Nature Publishing Group, pp. 229–233. ISSN: 1476-4687. DOI: 10.1038/nature11620. URL: <https://www.nature.com/articles/nature11620> (visited on 01/26/2024).
- [5] Johannes Hillbrand et al. “Coherent injection locking of quantum cascade laser frequency combs”. en. In: *Nature Photonics* 13.2 (Feb. 2019). Number: 2 Publisher: Nature Publishing Group, pp. 101–104. ISSN: 1749-4893. DOI: 10.1038/s41566-018-0320-3. URL: <https://www.nature.com/articles/s41566-018-0320-3> (visited on 01/31/2024).
- [6] Francesco Cappelli et al. “Frequency stability characterization of a quantum cascade laser frequency comb”. In: *Laser & Photonics Reviews* 10.4 (2016), pp. 623–630. ISSN: 1863-8899. DOI: 10.1002/lpor.201600003. URL: <https://onlinelibrary.wiley.com/doi/abs/10.1002/lpor.201600003> (visited on 12/06/2024).
- [7] Luigi Consolino et al. “Fully phase-stabilized quantum cascade laser frequency comb”. en. In: *Nature Communications* 10.1 (July 2019). Number: 1 Publisher: Nature Publishing Group, p. 2938. ISSN:

- 2041-1723. DOI: 10.1038/s41467-019-10913-7. URL: <https://www.nature.com/articles/s41467-019-10913-7> (visited on 01/31/2024).
- [8] K. N. Komagata et al. “Absolute frequency referencing in the long wave infrared using a quantum cascade laser frequency comb”. EN. In: *Optics Express* 30.8 (Apr. 2022). Publisher: Optica Publishing Group, pp. 12891–12901. ISSN: 1094-4087. DOI: 10.1364/OE.447650. URL: <https://opg.optica.org/oe/abstract.cfm?uri=oe-30-8-12891> (visited on 12/06/2024).
- [9] Jie Liu et al. “Field deployment of a multi-pass cell based mid-IR quantum cascade laser dual-comb spectrometer”. In: *Conference on Lasers and Electro-Optics*. Optica Publishing Group, 2021, AW2S.1. DOI: 10.1364/CLEO_AT.2021.AW2S.1. URL: https://opg.optica.org/abstract.cfm?URI=CLEO_AT-2021-AW2S.1.
- [10] P. Werle, R. Mücke, and F. Slemr. “The limits of signal averaging in atmospheric trace-gas monitoring by tunable diode-laser absorption spectroscopy (TDLAS)”. en. In: *Applied Physics B* 57.2 (Aug. 1993), pp. 131–139. ISSN: 1432-0649. DOI: 10.1007/BF00425997. URL: <https://doi.org/10.1007/BF00425997> (visited on 12/07/2024).
- [11] S.C. Gupta. “Phase-locked loops”. In: *Proceedings of the IEEE* 63.2 (Feb. 1975), pp. 291–306. ISSN: 1558-2256. DOI: 10.1109/PROC.1975.9735. URL: <https://ieeexplore.ieee.org/abstract/document/1451665> (visited on 04/28/2025).
- [12] Katarzyna Balakier et al. “Integrated Semiconductor Laser Optical Phase Lock Loops”. In: *IEEE Journal of Selected Topics in Quantum Electronics* 24.1 (Jan. 2018), pp. 1–12. ISSN: 1558-4542. DOI: 10.1109/JSTQE.2017.2711581. URL: <https://ieeexplore.ieee.org/document/7938320/> (visited on 04/28/2025).
- [13] J. Westberg, L. A. Sterczewski, and G. Wysocki. “Mid-infrared multiheterodyne spectroscopy with phase-locked quantum cascade lasers”. In: *Applied Physics Letters* 110.14 (Apr. 2017), p. 141108. ISSN: 0003-6951. DOI: 10.1063/1.4979825. URL: <https://doi.org/10.1063/1.4979825> (visited on 04/28/2025).